DISCRETE AND CONTINUOUS
DYNAMICAL SYSTEMS SERIES B
Volume **24**, Number **9**, September **2019**

doi:10.3934/dcdsb.2019032

pp. **4815–4826**

COMPARING MOTION OF CURVES AND HYPERSURFACES IN $\mathbb{R}^m$

Jiří Minarčík*

Department of Mathematics, Faculty of Nuclear Sciences and Physical Engineering
Czech Technical University in Prague
Trojanova 13
Prague, 12000, Czech Republic

Masato Kimura

Faculty of Mathematics and Physics
Kanazawa University
Kakuma
Kanazawa, 920-1192, Japan

Michal Beneš

Department of Mathematics, Faculty of Nuclear Sciences and Physical Engineering
Czech Technical University in Prague
Trojanova 13
Prague, 12000, Czech Republic

(Communicated by Shin-Ichiro Ei)

Abstract. This article aims to contribute to the understanding of the curvature flow of curves in a higher-dimensional space. Evolution of curves in $\mathbb{R}^m$ by their curvature is compared to the motion of hypersurfaces with constrained normal velocity. The special case of shrinking hyperspheres is further analyzed both theoretically and numerically by means of a semi-discrete scheme with discretization based on osculating circles. Computational examples of evolving spherical curves are provided along with the measurement of the experimental order of convergence.

1. **Introduction.** In physics, hypersurfaces and curves (mainly in $\mathbb{R}^3$), describe interfaces between different phases, defects in crystalline structure of materials or boundaries of thin layers (see [23, 19]). Their motion by curvature in various sense has been thoroughly studied, namely in two-dimensional case, where important theoretical results were obtained in [11, 10]. Modifications of curvature flow can

2010 *Mathematics Subject Classification.* Primary: 53C44, 14Q05, 14J70; Secondary: 34K12, 35B51.

Key words and phrases. Curvature flow, moving hypersurfaces, comparison principle, spherical curves, signed distance function.

Short acknowledgement.

The first and third author were partly supported by the project No. 15-27178A of Ministry of Health of the Czech Republic, the first author was partly supported by the Foundation Nadání Josefa, Marie a Zdeňky Hlávkových, by the Study at KU Scholarship from Kanazawa University and by the project of the Student Grant Agency of the Czech Technical University in Prague No. SGS17/194/OHK4/3T/14, and the second author was partly supported by JSPS KAKENHI Grant Numbers 15H03632 and 16H03953.

* Corresponding author: Jiří Minarčík.

be found in applications ranging from physics to computer image processing (see [18, 4, 22]). Various generalizations led to the mean curvature flow of hypersurfaces, studied in e.g. [14], or the motion of differentiable manifolds with higher codimension (see [24, 1]). Some of the classical results, however, do not hold under generalized circumstances. For instance, the comparison principle for two initially disjoint closed shrinking curves states that they can not intersect during the curvature flow. But curves in a space with higher dimension than 2 do not generally obey this rule and can adopt more complicated mutual positions. To understand principles of this curve motion, we analyze mutual position of an evolving curve and of an evolving hypersurface and find a comparison principle for it.

In this way, we achieve a new result which complements the features obtained in [7, 12, 15, 24]. The comparison principle proved in this article can also be used to recover properties of spherical curves presented in [12].

Curve evolution can be followed by means of several different approaches. In this contribution, we explore the parametric (direct) approach since it has a straightforward generalization from $\mathbb{R}^2$ to higher-dimensional spaces. Other approaches, such as the phase field or the level set method (see [22, 20]), are better suited for planar curves. Generalization of these methods for manifolds with higher codimension can be found in [5, 3]. In general, the parametric approach is less computationally demanding but, unlike other mentioned methods, it does not handle topological changes well.

The article is organized as follows. Section 2 introduces the curvature flow in arbitrary dimensional Euclidean space and includes the necessary notation for the parametric formulation. Similarly, the problems of moving hypersurfaces are introduced in Section 3. The main theoretical result and its proof is provided in Section 4. The consequences of the main theorem are discussed in Section 5. Section 6 describes a semi-discrete numerical scheme for the curvature flow in arbitrary dimensional space with discretization based on osculating circles. The last section includes computational examples that demonstrate the behavior of spherical curves under the curvature flow.

2. Parametric description of moving curves in $\mathbb{R}^m$.

We study the curvature flow of closed curves in $\mathbb{R}^m$ by means of the parametric approach. For this purpose, we introduce the following notation.

Let $\{\Gamma_t\}_{t\in[0,T_\Gamma)}$ be a family of closed curves in $\mathbb{R}^m$ evolving in time interval $[0,T_\Gamma)$. For given $t \in [0,T_\Gamma)$, the curve Γ_t is represented by a parametrization $\mathbf{X}(\cdot,t) : \mathbb{S}^1 \to \mathbb{R}^m$. We make the following regularity assumptions on $\mathbf{X}$:

$$\mathbf{X} \in \mathcal{C}^1(\mathbb{S}^1 \times [0,T_\Gamma);\mathbb{R}^m), \tag{1}$$

$$\mathbf{X}(\cdot,t) \in \mathcal{C}^2(\mathbb{S}^1;\mathbb{R}^m) \text{ for all } t \in [0,T_\Gamma), \tag{2}$$

$$|\partial_u \mathbf{X}(u,t)| > 0 \text{ for all } u \in \mathbb{S}^1 \text{ and } t \in [0,T_\Gamma). \tag{3}$$

Here $\mathbb{S}^1 = \mathbb{R}/2\pi\mathbb{Z}$ is a unit circle and $|\cdot|$ is the Euclidean norm in $\mathbb{R}^m$.

The tangent vector $\mathbf{T}(u,t)$ and the curvature $K(u,t)$ are defined as

$$\mathbf{T}(u,t) = |\partial_u \mathbf{X}(u,t)|^{-1}\partial_u \mathbf{X}(u,t), \qquad K(u,t) = |\partial_u \mathbf{X}(u,t)|^{-1}|\partial_u \mathbf{T}(u,t)|.$$

for all $u \in \mathbb{S}^1$ and $t \in [0,T_\Gamma)$. The principal normal vector $\mathbf{N}(u,t)$ is defined only when $K(u,t) > 0$ as $\mathbf{N}(u,t) = |\partial_u \mathbf{T}(u,t)|^{-1}\partial_u \mathbf{T}(u,t)$.

The time evolution of $\{\Gamma_t\}_{t\in[0,T_\Gamma)}$ is given by the curvature flow in the form of the initial-value problem for the paramerization $\mathbf{X} = \mathbf{X}(u,t)$:

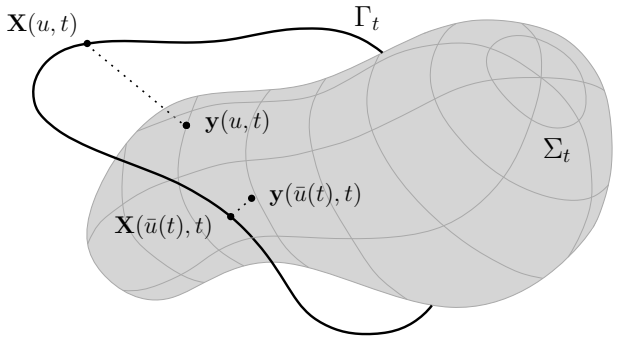

FIGURE 1. Visualization for the definition of $\mathbf{y}(u,t)$ and $\bar{u}(t)$.

$$\partial_t \mathbf{X} = K\mathbf{N} \qquad \text{in } \mathbb{S}^1 \times (0, T_\Gamma), \tag{4}$$

$$\mathbf{X}|_{t=0} = \mathbf{X}_{ini} \qquad \text{in } \mathbb{S}^1, \tag{5}$$

where $\mathbf{X}_{ini} \in \mathcal{C}^2(\mathbb{S}^1; \mathbb{R}^m)$ describes the initial curve Γ_0. Although $\mathbf{N}$ is undefined at the points of Γ_t where $K = 0$, the term $K\mathbf{N} = |\partial_u \mathbf{X}|^{-1} \partial_u \mathbf{T}$ in (4) is defined everywhere.

The existence of the solution for (4-5) together with analysis of singularities and behavior of global quantities was studied for curves in $\mathbb{R}^3$ by Altschuler in [1, 2] and later for curves in spaces with higher dimension in [24].

3. **Moving hypersurfaces in $\mathbb{R}^m$ and the signed distance function.** In this contribution, we aim to compare evolution of $\{\Gamma_t\}_{t\in[0,T_\Gamma)}$ and evolution of a hypersurface given by its normal velocity. To this end, we introduce the notion of moving hypersurface as follows.

Let $\{\Sigma_t\}_{t\in[0,T_\Sigma)}$ be a family of closed oriented $\mathcal{C}^2$-class hypersurfaces in $\mathbb{R}^m$ evolving in the time interval $[0, T_\Sigma)$. Since, for a given $t \in [0, T_\Sigma)$, Σ_t is an oriented and closed manifold, we can define two disjoint open sets $\Omega_t^\pm$ such that $\Omega_t^+ \cup \Omega_t^- = \mathbb{R}^m \setminus \Sigma_t$. The unit normal vector of Σ_t at the point $\mathbf{y} \in \Sigma_t$ is denoted by $\boldsymbol{\nu}(\mathbf{y}, t)$ and it is always pointing outward of Ω_t^+. The extended Weingarten map is defined as $W(\mathbf{y}, t) = -(\nabla_{\Sigma_t}\nu_1, \dots, \nabla_{\Sigma_t}\nu_m)(\mathbf{y}, t)$, where ∇_{Σ_t} is the surface gradient on Σ_t. The principal curvatures $\kappa_1, \dots, \kappa_{m-1}$ are the eigenvalues of W with $\mathbf{e}_i \cdot \boldsymbol{\nu} = 0$, i.e. $W\mathbf{e}_i = \kappa_i \mathbf{e}_i$ for $i = 1, \dots, m-1$ and $W\boldsymbol{\nu} = \mathbf{0}$. We remark that $\{\mathbf{e}_1, \dots, \mathbf{e}_{m-1}, \boldsymbol{\nu}\}$ becomes an orthonormal basis of $\mathbb{R}^m$ (see Chapter 2 in [16] for further detail).

Let us define

$$\mathcal{M} := \bigcup_{t\in[0,T_\Sigma)} \Sigma_t \times \{t\} \subset \mathbb{R}^m \times \mathbb{R}.$$

Following the notation in Chapter 5 from [16], we call $\{\Sigma_t\}_{t\in[0,T_\Sigma)}$ a $\mathcal{C}^{2,1}$-class if $\boldsymbol{\nu} \in \mathcal{C}^1(\mathcal{M}; \mathbb{R}^m)$.

Note that changing the orientation of Σ_t, i.e. swapping Ω_t^+ and Ω_t^-, affects the direction of the normal vector $\boldsymbol{\nu}$ as well as the sign of the principal curvatures κ_i. For instance, if we consider $\Sigma_t = \partial B$ and $\Omega_t^- = B$, where B is a unit ball in $\mathbb{R}^m$, the normal vector $\boldsymbol{\nu}$ is pointing towards the center of B and all principal curvature are equal to 1.

The time evolution of $\{\Sigma_t\}_{t\in[0,T_\Sigma)}$ is given by specifying its normal velocity $v(\mathbf{x},t) = \mathbf{z}'(t)\cdot\boldsymbol{\nu}(\mathbf{x},t)$, where $\mathbf{z}$ is any differentiable function with respect to t such that $\mathbf{z}(0)=\mathbf{x}$ and $\mathbf{z}(t')\in\Sigma_{t'}$ for all t' from some neighborhood of t.

When analyzing the relationship of the curve Γ_t evolved by (4-5) and of a moving hypersurface, we explore the tools such as the signed-distance function. Relationship of a point $\mathbf{x}\in\mathbb{R}^m$ to Σ_t is provided by the signed-distance function defined as follows

$$d(\mathbf{x},t) := \begin{cases} \operatorname{dist}(\mathbf{x},\Sigma_t) & \text{for } \mathbf{x}\in\Omega_t^+ \\ 0 & \text{for } \mathbf{x}\in\Sigma_t \\ -\operatorname{dist}(\mathbf{x},\Sigma_t) & \text{for } \mathbf{x}\in\Omega_t^- \end{cases}.$$

We use the following notation (see Figure 1):

$$\mathbf{y}(u,t) = \operatorname*{argmin}_{\mathbf{y}\in\Sigma_t} |\mathbf{X}(u,t)-\mathbf{y}|,$$
$$\bar{u}(t) = \operatorname*{argmin}_{u\in\mathbb{S}^1} |\mathbf{X}(u,t)-\mathbf{y}(u,t)|.$$

The following remark contains useful formulae for the signed-distance function. They are shown in Chapter 3 from [16].

Remark 1. When Σ_t is sufficiently smooth, there exists $\varepsilon_0>0$ such that when $\operatorname{dist}(\mathbf{X}(u,t),\Sigma_t)<\varepsilon_0$ for some $u\in\mathbb{S}^1$ and $t\in[0,T_\Sigma)$, then $\mathbf{y}(u,t)$ is unique and the signed distance function d satisfies

$$\nabla d(\mathbf{X}(u,t),t) = -\boldsymbol{\nu}(\mathbf{y}(u,t),t), \tag{6}$$

$$\Delta d(\mathbf{X}(u,t),t) = \sum_{i=1}^{m-1} \frac{\kappa_i(\mathbf{y}(u,t),t)}{1+d(\mathbf{X}(u,t),t)\kappa_i(\mathbf{y}(u,t),t)}, \tag{7}$$

$$\mathbb{H}d(\mathbf{X}(u,t),t) = (I+d(\mathbf{X}(u,t))W(\mathbf{y}(u,t),t))^{-1}W(\mathbf{y}(u,t),t), \tag{8}$$

$$\partial_t d(\mathbf{X}(u,t),t) = v(\mathbf{y}(u,t),t). \tag{9}$$

where $\mathbb{H}d|_{i,j} = \frac{\partial^2 d}{\partial x_i \partial x_j}$ for $i,j\le m$ is the Hessian matrix of d and I is the identity matrix of size m.

4. Generalized comparison principle.

In the following, we study the relationship between the moving hypersurface Σ_t introduced in Section 3 and the moving curve given by (4-5) which for $t=0$ is on one side of Σ_0. We show that it remains to be so for a time span given by the assumptions.

For $t\in[0,\min\{T_\Gamma,T_\Sigma\})$ we introduce the function

$$R(t) := \min_{u\in\mathbb{S}^1} \operatorname{dist}(\mathbf{X}(u,t),\Sigma_t) = \operatorname{dist}(\mathbf{X}(\bar{u}(t),t),\Sigma_t) = |\mathbf{X}(\bar{u}(t),t)-\mathbf{y}(\bar{u}(t),t)| \tag{10}$$

describing the distance of both sets. Our main result is contained in the following statement.

Main Theorem. *Let $\{\Sigma_t\}_{t\in[0,T_\Sigma)}$ be a $\mathcal{C}^{2,1}$-class moving hypersurface with normal velocity satisfying*

$$v(\mathbf{y},t) \ge \max_{1\le i<m} \kappa_i(\mathbf{y},t) \tag{11}$$

for all $t\in[0,T_\Sigma)$ and all $\mathbf{y}\in\Sigma_t$. Let Γ_t satisfy (1-3) and evolve according to (4-5) with the initial condition $\Gamma_0\subset\Omega_0^+$ and $\mathbf{X}_{ini}\in\mathcal{C}^2(\mathbb{S}^1;\mathbb{R}^m)$.

We suppose that there exists $\varepsilon_0>0$ such that, for all $u\in\mathbb{S}^1$ and $t\in[0,T_\Sigma)$ for which $0<\operatorname{dist}(\mathbf{X}(u,t),\Sigma_t)<\varepsilon_0$, there exist $\mathbf{y}(u,t)$ and $\bar{u}(t)$ and equations (6-9)

are satisfied. Furthermore, assume that both the normal velocity v of Σ_t and the curvature K of Γ_t are uniformly bounded on $[0, \min\{T_\Gamma, T_\Sigma\})$. Then

$$\forall t \in [0, \min\{T_\Gamma, T_\Sigma\}) : \ R(t) \geq \min\{\varepsilon_0, R(0)\}. \tag{12}$$

Proof. According to (10), we abbreviate $\bar{\mathbf{X}}(t) := \mathbf{X}(\bar{u}(t), t)$, $\bar{\mathbf{y}}(t) := \mathbf{y}(\bar{u}(t), t)$ and denote

$$I_\varepsilon := \{t \in [0, \min\{T_\Gamma, T_\Sigma\}) \ : \ \operatorname{dist}(\bar{\mathbf{X}}(t), \Sigma_t) < \varepsilon\}$$

for a particular $\varepsilon > 0$. Now set $\varepsilon = \varepsilon_0$ from Remark 1 from which the formulae (6-9) hold on I_{ε_0}. As $d(\mathbf{X}(\cdot, t), t)$ attains its minimum at the point $\bar{u}(t)$ and is twice differentiable, we have

$$0 = \tfrac{\mathrm{d}}{\mathrm{d}u} \left[d(\mathbf{X}(u,t),t) \right] |_{u=\bar{u}(t)} = \nabla d(\bar{\mathbf{X}}(t), t) \cdot \partial_u \mathbf{X}(\bar{u}(t), t) \tag{13}$$

and

$$\begin{aligned} 0 \leq \tfrac{\mathrm{d}^2}{\mathrm{d}u^2} \left[d(\mathbf{X}(u,t),t) \right] |_{u=\bar{u}(t)} &= \tfrac{\mathrm{d}}{\mathrm{d}u} \left[\nabla d(\mathbf{X}(u,t),t) \cdot \partial_u \mathbf{X}(u,t) \right] |_{u=\bar{u}(t)} \\ &= [\mathbb{H} d(\bar{\mathbf{X}}(t), t) \partial_u \mathbf{X}(\bar{u}(t), t)] \cdot \partial_u \mathbf{X}(\bar{u}(t), t) + \nabla d(\bar{\mathbf{X}}(t), t) \cdot \partial_u^2 \mathbf{X}(\bar{u}(t), t), \end{aligned} \tag{14}$$

where

$$\partial_u \mathbf{X}(u,t) = |\partial_u \mathbf{X}(u,t)| \mathbf{T}(u,t),$$
$$\partial_u^2 \mathbf{X}(u,t) = |\partial_u \mathbf{X}(u,t)|^{-1} \partial_u |\partial_u \mathbf{X}(u,t)| \partial_u \mathbf{X}(u,t) + |\partial_u \mathbf{X}(u,t)|^2 K(u,t) \mathbf{N}(u,t).$$

From (6) and (13), it follows that $\mathbf{T}(\bar{u}(t), t) \cdot \boldsymbol{\nu}(\mathbf{y}(t), t) = 0$. Moreover,

$$\nabla d(\bar{\mathbf{X}}(t), t) \cdot \partial_u^2 \mathbf{X}(\bar{u}(t), t) = -|\partial_u \mathbf{X}(\bar{u}(t), t)|^2 \boldsymbol{\nu}(\bar{\mathbf{y}}(t), t) \cdot (K\mathbf{N})(\bar{u}(t), t). \tag{15}$$

Substitution of (15) to (14) yields

$$[\mathbb{H} d(\bar{\mathbf{X}}(t), t) \mathbf{T}(\bar{u}(t), t)] \cdot \mathbf{T}(\bar{u}(t), t) - \boldsymbol{\nu}(\bar{\mathbf{y}}(t), t) \cdot (K\mathbf{N})(\bar{u}(t), t) \geq 0. \tag{16}$$

In the second part of the proof, we show that the function R, introduced in (10), is Lipschitz continuous in I_{ε_0}. The definition of $\bar{u}(t)$ implies

$$\begin{aligned} R(t_2) - R(t_1) &= d(\mathbf{X}(\bar{u}(t_2), t_2), t_2) - d(\mathbf{X}(\bar{u}(t_1), t_1), t_1) \\ &\leq d(\mathbf{X}(\bar{u}(t_1), t_2), t_2) - d(\mathbf{X}(\bar{u}(t_1), t_1), t_1). \end{aligned}$$

From properties of $d(\mathbf{X}(u,t),t)$, there is a constant $C > 0$ such that for any fixed $u \in \mathbb{S}^1$ and for all $t \in I_{\varepsilon_0}$ we have

$$\begin{aligned} \left| \tfrac{\mathrm{d}}{\mathrm{d}t} d(\mathbf{X}(u,t),t) \right| &= |\nabla d(\mathbf{X}(u,t),t) \cdot \partial_t \mathbf{X}(u,t) + \partial_t d(\mathbf{X}(u,t),t)| \\ &\leq |\nabla d(\mathbf{X}(u,t),t) \cdot K(u,t) \mathbf{N}(u,t)| + |v(\mathbf{y}(u,t),t)| \\ &\leq \sup_{t \in [0, \min\{T_\Gamma, T_\Sigma\})} \left(\max_{u \in \mathbb{S}^1} |K(u,t)| + \max_{\mathbf{y} \in \Sigma_t} |v(\mathbf{y},t)| \right) =: C \end{aligned}$$

due to the assumptions of Main Theorem. Thus $|R(t_2) - R(t_1)| \leq C|t_2 - t_1|$. The Rademacher theorem (see [9]) implies the existence of a subset $N \subset I_{\varepsilon_0}$ with zero one-dimensional Lebesgue measure $\mu(N) = 0$ such that for all $t \in I_{\varepsilon_0} \setminus N =: \tilde{I}_{\varepsilon_0}$ we have

$$R'(t) = \lim_{h \to 0^+} \frac{R(t+h) - R(t)}{h} = \lim_{h \to 0^+} \frac{R(t) - R(t-h)}{h} \leq C.$$

For $t \in \tilde{I}_{\varepsilon_0}$ and small $h > 0$ we have

$$\begin{aligned} R(t+h) - R(t) &\leq d(\mathbf{X}(\bar{u}(t), t+h), t+h) - d(\mathbf{X}(\bar{u}(t), t), t) \\ \text{and } R(t) - R(t-h) &\geq d(\mathbf{X}(\bar{u}(t), t), t) - d(\mathbf{X}(\bar{u}(t), t-h), t-h). \end{aligned}$$

Dividing by h and letting $h \to 0^+$ yields $R'(t) \leq \frac{\mathrm{d}}{\mathrm{d}t} d(\mathbf{X}(u,t),t)|_{u=\bar{u}(t)}$ and $R'(t) \geq \frac{\mathrm{d}}{\mathrm{d}t} d(\mathbf{X}(u,t),t)|_{u=\bar{u}(t)}$. Thus we obtain equality

$$\begin{aligned} R'(t) &= \tfrac{\mathrm{d}}{\mathrm{d}t} d(\mathbf{X}(u,t),t)|_{u=\bar{u}(t)} = \nabla d(\bar{\mathbf{X}}(t),t) \cdot \partial_t \mathbf{X}(\bar{u}(t),t) + \partial_t d(\bar{\mathbf{X}}(t),t) \\ &= -\boldsymbol{\nu}(\bar{\mathbf{y}}(t),t) \cdot (K\mathbf{N})(\bar{u}(t),t) + v(\bar{\mathbf{y}}(t),t). \end{aligned}$$

From (16) and the assumption (11), we get

$$R'(t) \geq -[\mathbb{H} d(\bar{\mathbf{X}}(t),t)\mathbf{T}(\bar{u}(t),t)] \cdot \mathbf{T}(\bar{u}(t),t) + \max_{1 \leq i < m} \kappa_i(\bar{\mathbf{y}}(t),t).$$

The first term can be rewritten as

$$\begin{aligned} &[\mathbb{H} d(\bar{\mathbf{X}}(t),t)\mathbf{T}(\bar{u}(t),t)] \cdot \mathbf{T}(\bar{u}(t),t) \\ &\qquad = [(I + d(\bar{\mathbf{X}}(t),t)W(\bar{\mathbf{y}}(t),t))^{-1} W(\bar{\mathbf{y}}(t),t)\mathbf{T}(\bar{u}(t),t)] \cdot \mathbf{T}(\bar{u}(t),t) \\ &\qquad = \sum_{i=1}^{m-1} [\mathbf{T}(\bar{u}(t),t) \cdot \mathbf{e}_i(\bar{\mathbf{y}}(t),t)]^2 \frac{\kappa_i(\bar{\mathbf{y}}(t),t)}{1 + d(\bar{\mathbf{X}}(t),t)\kappa_i(\bar{\mathbf{y}}(t),t)}. \end{aligned}$$

Since $d(\bar{\mathbf{X}}(t),t)$ is non-negative, we have

$$\frac{\kappa_i(\bar{\mathbf{y}}(t),t)}{1 + d(\bar{\mathbf{X}}(t),t)\kappa_i(\bar{\mathbf{y}}(t),t)} \leq \kappa_i(\bar{\mathbf{y}}(t),t) \leq \max_{1 \leq j < m} \kappa_j(\bar{\mathbf{y}}(t),t).$$

Thus, since $\{\mathbf{e}_1, \ldots, \mathbf{e}_{m-1}, \boldsymbol{\nu}\}$ is an orthonormal basis, we obtain

$$R'(t) \geq \left(-\sum_{i=1}^{m-1} [\mathbf{T}(\bar{u}(t),t) \cdot \mathbf{e}_i(\bar{\mathbf{y}}(t),t)]^2 + 1 \right) \max_{1 \leq i < m} \kappa_i(\bar{\mathbf{y}}(t),t) = 0.$$

We can define $c_0 := \min\{\varepsilon_0, R(0)\} > 0$, where $R(0) > 0$ follows from the assumption $\Gamma_0 \subset \Omega_0^+$. We prove (12) by contradiction. Assume there would exist time $t_1 \in (0, \min\{T_\Gamma, T_\Sigma\})$ such that $R(t_1) \in (0, c_0)$ and $R(t_1) \leq R(t)$ for $t \in [0, t_1]$. Since the function R is continuous on $[0, \min\{T_\Gamma, T_\Sigma\})$, we can find $t_0 \in [0, t_1)$ satisfying

$$R(t_1) < R(t_0) \quad \text{and} \quad R(t) < \varepsilon_0 \text{ for } t \in [t_0, t_1]. \tag{17}$$

Because $R' \geq 0$ almost everywhere on $[t_0, t_1]$, we would get

$$R(t_1) - R(t_0) = \int_{t_0}^{t_1} R'(t) \mathrm{d}t \geq 0.$$

This contradicts (17). Hence we conclude that $R(t) \geq c_0$. □

Remark 2. Note that for $m = 2$, Main Theorem reduces to the classical result from [11, 10]. Namely, two initially disjoint planar curves moving according to the curvature flow cannot intersect.

5. **Applications.** The previous result has the following straightforward consequences.

Corollary 1. *Let Γ_t evolve according to (4-5) with the initial condition Γ_0 satisfying $\Gamma_0 \cap \partial B(\mathbf{x_0}, r_0) = \varnothing$ for some $\mathbf{x_0} \in \mathbb{R}^m$ and $r_0 > 0$. Then*

$$\forall t \in \left[0, \min\left\{T_\Gamma, \tfrac{1}{2} r_0^2\right\}\right) : \ \Gamma(t) \cap \partial B\left(\mathbf{x_0}, \sqrt{r_0^2 - 2t}\right) = \varnothing.$$

In particular, if $\Gamma_0 \subset B(\mathbf{x}_0, r_0)$, $T_\Gamma \leq \frac{1}{2} r_0^2$ has to be satisfied.

Proof. Let $\Sigma_t := \partial B\left(\mathbf{x_0}, \sqrt{r_0^2 - 2t}\right)$ with the orientation defined by position of Γ_0 as $\Gamma_0 \subset \Omega_0^+$. The hypersurface Σ_t evolves according to its mean curvature as

$$v = \max_{1\le i\le m} \kappa_i = \pm(r_0^2 - 2t)^{-\frac{1}{2}},$$

where the sign is given by the orientation of Σ_t. Main Theorem guarantees that $\Gamma_t \subset \Omega_t^+$ for all $t \in \left[0, \min\left\{T_\Gamma, \frac{1}{2}r_0^2\right\}\right)$. □

In the following, we provide an alternative proof of the fact that spherical curves remain spherical under the curvature flow. The original proof is from [12] and simple implications of this statement can be found in [7, 15].

Corollary 2. *Let Γ_t evolve according to (4-5) with the initial condition Γ_0 satisfying $\Gamma_0 \subset \partial B(\mathbf{x_0}, r_0)$ for some $\mathbf{x_0} \in \mathbb{R}^m$ and $r_0 > 0$. Then*

$$\forall t \in \left[0, \min\left\{T_\Gamma, \tfrac{1}{2}r_0^2\right\}\right) : \ \Gamma_t \subset \partial B\left(\mathbf{x_0}, \sqrt{r_0^2 - 2t}\right).$$

Proof. The Corollary 1 allows us to bound Γ_t between two spheres

$$\Gamma_t \subset B\left(\mathbf{x_0}, \sqrt{r_0^2 + \varepsilon - 2t}\right) \setminus \bar{B}\left(\mathbf{x_0}, \sqrt{r_0^2 - \varepsilon - 2t}\right),$$

where $0 < \varepsilon < r_0^2$ and $t \in \left[0, \min\left\{T_\Gamma, \frac{1}{2}(r_0^2 - \varepsilon)\right\}\right)$. Passing ε to 0 proves the statement. □

Corollary 3. *Let Γ_t evolve according to (4-5) with the initial condition Γ_0 satisfying $\Gamma_0 \subset \Omega$, where $\Omega \subset \mathbb{R}^n$ is a bounded convex set with a $\mathcal{C}^2$-class boundary $\partial\Omega$. Then*

$$\forall t \in [0, T_\Gamma) : \ \Gamma_t \subset \Omega.$$

Proof. The convexity of Ω allows for a trivial choice of the moving hypersurface $\Sigma_t := \partial\Omega$ with the normal velocity $v \equiv 0$. The assumption (11) from Main Theorem is satisfied because all principal curvatures of $\partial\Omega$ are non-positive. □

6. **Numerical approximation.** The curvature flow of curves in $\mathbb{R}^m$ can be numerically treated in a way similar to [17]. First, we discretize spatial derivatives by means of the osculating circles and then solve the resulting system of time-dependent ODE's by means of the Runge-Kutta-Merson scheme.

A discrete curve $\tilde{\Gamma}$ is a finite set of nodes $\{\tilde{\mathbf{X}}_i\}_{i=0}^{N-1}$ connected by linear segments, where $N \in \mathbb{N}$ is the number of nodes. In order to simplify further notation for closed curves, we set $\tilde{\mathbf{X}}_{-1} := \tilde{\mathbf{X}}_{N-1}$ and $\tilde{\mathbf{X}}_N := \tilde{\mathbf{X}}_0$. The vector $K\mathbf{N}$ can be approximated by means of the geometrical approach based on osculating circles. The approximate values of K and $\mathbf{N}$ at the node $\tilde{\mathbf{X}}_i$ are denoted by $\tilde{K}_i$ and $\tilde{\mathbf{N}}_i$, respectively.

Consider a particular node $\tilde{\mathbf{X}}_i \in \tilde{\Gamma}$, where $0 \le i < N$. We define

$$\mathbf{u} := \tilde{\mathbf{X}}_i - \tilde{\mathbf{X}}_{i-1}, \qquad \tilde{\mathbf{X}}_{i-\frac{1}{2}} := \tfrac{1}{2}(\tilde{\mathbf{X}}_{i-1} + \tilde{\mathbf{X}}_i),$$
$$\mathbf{v} := \tilde{\mathbf{X}}_{i+1} - \tilde{\mathbf{X}}_i, \qquad \tilde{\mathbf{X}}_{i+\frac{1}{2}} := \tfrac{1}{2}(\tilde{\mathbf{X}}_i + \tilde{\mathbf{X}}_{i+1}),$$

as shown in Figure 2. In order to approximate the curvature K, we find the center $\mathbf{S}$ of the circle c defined by the points $\tilde{\mathbf{X}}_{i-1}$, $\tilde{\mathbf{X}}_i$ and $\tilde{\mathbf{X}}_{i+1}$. Since c is the circumscribed circle of the triangle with the vertices $\tilde{\mathbf{X}}_{i-1}$, $\tilde{\mathbf{X}}_i$ and $\tilde{\mathbf{X}}_{i+1}$ and lies in the osculating plane, the point $\mathbf{S}$ has to satisfy the following conditions:

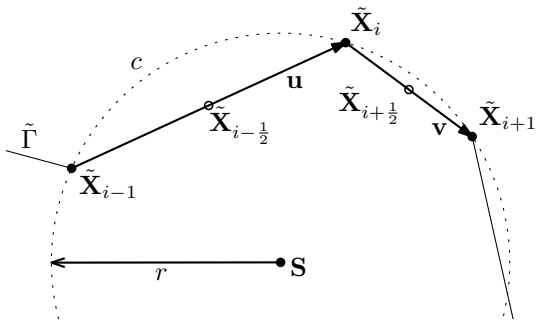

FIGURE 2. Visualization of the geometric quantities defined in the osculating plane.

$$\mathbf{S} - \tilde{\mathbf{X}}_i \in \{\mathbf{u}, \mathbf{v}\}_{span}, \tag{18}$$

$$\mathbf{S} - \tilde{\mathbf{X}}_{i-\frac{1}{2}} \perp \mathbf{u}, \tag{19}$$

$$\mathbf{S} - \tilde{\mathbf{X}}_{i+\frac{1}{2}} \perp \mathbf{v}. \tag{20}$$

First condition (18) implies the existence of $t_1, t_2 \in \mathbb{R}$, such that $\mathbf{S} = \tilde{\mathbf{X}}_i + t_1\mathbf{u} + t_2\mathbf{v}$. This allows us to rewrite (19) and (20) as

$$(\mathbf{S} - \tilde{\mathbf{X}}_{i-\frac{1}{2}}) \cdot \mathbf{u} = t_1|\mathbf{u}|^2 + t_2\mathbf{v}\cdot\mathbf{u} - (\tilde{\mathbf{X}}_{i-\frac{1}{2}} - \tilde{\mathbf{X}}_i)\cdot\mathbf{u} = 0,$$
$$(\mathbf{S} - \tilde{\mathbf{X}}_{i+\frac{1}{2}}) \cdot \mathbf{v} = t_1\mathbf{u}\cdot\mathbf{v} + t_2|\mathbf{v}|^2 - (\tilde{\mathbf{X}}_{i+\frac{1}{2}} - \tilde{\mathbf{X}}_i)\cdot\mathbf{v} = 0.$$

The parameters t_1 and t_2 can be obtained by solving the following linear system:

$$\mathbb{A}\cdot\begin{pmatrix} t_1 \\ t_2 \end{pmatrix} := \begin{pmatrix} |\mathbf{u}|^2 & \mathbf{u}\cdot\mathbf{v} \\ \mathbf{u}\cdot\mathbf{v} & |\mathbf{v}|^2 \end{pmatrix}\cdot\begin{pmatrix} t_1 \\ t_2 \end{pmatrix} = \begin{pmatrix} (\tilde{\mathbf{X}}_{i-\frac{1}{2}} - \tilde{\mathbf{X}}_i)\cdot\mathbf{u} \\ (\tilde{\mathbf{X}}_{i+\frac{1}{2}} - \tilde{\mathbf{X}}_i)\cdot\mathbf{v} \end{pmatrix} = \begin{pmatrix} -\frac{1}{2}|\mathbf{u}|^2 \\ \frac{1}{2}|\mathbf{v}|^2 \end{pmatrix}. \tag{21}$$

When $\det\mathbb{A} = |\mathbf{u}|^2|\mathbf{v}|^2 - (\mathbf{u}\cdot\mathbf{v})^2 = 0$, the points $\tilde{\mathbf{X}}_{i-1}$, $\tilde{\mathbf{X}}_i$ and $\tilde{\mathbf{X}}_{i+1}$ are collinear and we set $\tilde{K}_i := 0$. Otherwise, the system (21) has a unique solution

$$t_1 = -\frac{|\mathbf{v}|^2(|\mathbf{u}|^2 + \mathbf{u}\cdot\mathbf{v})}{2\det\mathbb{A}}, \qquad t_2 = \frac{|\mathbf{u}|^2(|\mathbf{v}|^2 + \mathbf{u}\cdot\mathbf{v})}{2\det\mathbb{A}}.$$

Then the curvature $\tilde{K}_i$ is calculated as the reciprocal of the radius r of the osculation circle c (see Figure 2)

$$\tilde{K}_i := \tfrac{1}{r} = |\tilde{\mathbf{X}}_i - \mathbf{S}|^{-1} = |t_1\mathbf{u} + t_2\mathbf{v}|^{-1}.$$

The principal normal vector $\mathbf{N}$ is approximated by the expression

$$\tilde{\mathbf{N}}_i := \tilde{K}_i(\mathbf{S} - \tilde{\mathbf{X}}_i).$$

Semi-discrete scheme. For numerical integration of the initial value problem

$$\frac{\mathrm{d}\tilde{\mathbf{X}}_i}{\mathrm{d}t} = \tilde{K}_i^2(\mathbf{S}_i - \tilde{\mathbf{X}}_i), \tag{22}$$

$$\tilde{\mathbf{X}}_i|_{t=0} = \mathbf{X}_{ini}\left(\frac{2\pi i}{N}\right), \tag{23}$$

we use the 4th order accurate Runge-Kutta-Merson method with an automatic time step adjustment as in [6].

Denoting $\tilde{\mathbf{X}} = (\tilde{\mathbf{X}}_0, \dots, \tilde{\mathbf{X}}_{N-1})$ and $\mathbf{F}_i(\tilde{\mathbf{X}}) = \tilde{K}_i \tilde{\mathbf{N}}_i$, system (22-23) has the following form

$$\tilde{\mathbf{X}}_i'(t) = \mathbf{F}_i(\tilde{\mathbf{X}}(t)).$$

We denote the time step $\tau > 0$ and the time level $\tilde{t}$. The next time level is given by the formula

$$\tilde{\mathbf{X}}(\tilde{t} + \tau) = \tilde{\mathbf{X}}(\tilde{t}) + \tfrac{1}{6}(\mathbf{k}_1 + 4\mathbf{k}_4 + \mathbf{k}_5),$$

where $\mathbf{k}_j = (\mathbf{k}_{j,0}, \dots, \mathbf{k}_{j,N-1})$ is given by

$$\begin{aligned}
\mathbf{k}_{1,i} &= \mathbf{F}_i(\tilde{\mathbf{X}}(\tilde{t})),\\
\mathbf{k}_{2,i} &= \mathbf{F}_i(\tilde{\mathbf{X}}(\tilde{t}) + \tfrac{\tau}{3}\mathbf{k}_1),\\
\mathbf{k}_{3,i} &= \mathbf{F}_i(\tilde{\mathbf{X}}(\tilde{t}) + \tfrac{\tau}{6}(\mathbf{k}_1 + \mathbf{k}_2)),\\
\mathbf{k}_{4,i} &= \mathbf{F}_i(\tilde{\mathbf{X}}(\tilde{t}) + \tfrac{\tau}{8}(\mathbf{k}_1 + 3\mathbf{k}_3)),\\
\mathbf{k}_{5,i} &= \mathbf{F}_i(\tilde{\mathbf{X}}(\tilde{t}) + \tfrac{\tau}{2}(\mathbf{k}_1 - 3\mathbf{k}_3 + 4\mathbf{k}_4)).
\end{aligned}$$

The time step τ is updated at each iteration as in [13], page 246.

$$\tau_{new} = \left(\frac{\delta}{\varepsilon}\right)^{\frac{1}{5}} \omega\tau, \qquad \text{where } \varepsilon = \max_{0\le i<N} \frac{1}{3}\left|\frac{1}{5}\mathbf{k}_{1,i} - \frac{9}{10}\mathbf{k}_{3,i} + \frac{4}{5}\mathbf{k}_{4,i} - \frac{1}{10}\mathbf{k}_{5,i}\right|.$$

The control parameters ω and δ must satisfy $0 < \omega < 1$ and $\delta > 0$.

7. **Numerical verification.** We include two computational examples serving both as verification of the numerical scheme and testing of the properties of moving spherical curves. According to Corollary 2, spherical curves under the curvature flow should remain embedded in a shrinking sphere.

We assume that Γ_0 is embedded in a unit sphere centered at the origins. The deviation of the discretized curve from the shrinking sphere radius is characterized by

$$\mathcal{E}_\infty(N) := \max_{\tilde{t}} \max_{0\le i<N} \left||\tilde{\mathbf{X}}_i(\tilde{t})| - \sqrt{1-2\tilde{t}}\right|,$$

$$\mathcal{E}_p(N) := \max_{\tilde{t}} \left(\frac{1}{L(\tilde{t})} \sum_{i=0}^{N-1} \frac{l_{i+1}(\tilde{t}) + l_i(\tilde{t})}{2} \left||\tilde{\mathbf{X}}_i(\tilde{t})| - \sqrt{1-2\tilde{t}}\right|^p\right)^{\frac{1}{p}},$$

where $p \in \mathbb{N}$, $L(\tilde{t}) := \sum_{i=0}^{N-1} l_i(\tilde{t})$ and $l_i(\tilde{t}) := \left|\tilde{\mathbf{X}}_i(\tilde{t}) - \tilde{\mathbf{X}}_{i-1}(\tilde{t})\right|$.

The Experimental Order of Convergence (EOC) used in [21, 8] is calculated as

$$\mathrm{EOC}_p(N_1, N_2) := \frac{\log \frac{\mathcal{E}_p(N_1)}{\mathcal{E}_p(N_2)}}{\log \frac{N_2}{N_1}},$$

where $p \in \mathbb{N}$ or $p = \infty$. The following numerical simulations were performed by using the semi-discrete scheme (22-23) with the control parameters $\delta = 10^{-5}$ and $\omega = 0.8$ as suggested in [13], page 246.

Example 1. The initial curve Γ_0 for the first example is given by the parametrization

$$\mathbf{X}\left(\tfrac{u+\pi}{2\pi}, 0\right) = \begin{pmatrix} \cos(6u)\sin u \\ \sin(6u)\sin|u| \\ -\cos u \end{pmatrix}, \qquad u \in [-\pi, \pi].$$

The results of the numerical simulation are presented in Table 1 and Figure 3.

TABLE 1. Results of the numerical computation from Example 1. The error measurements were taken during time interval $[0, 0.45]$.

N	$\mathcal{E}_\infty(N)$	EOC_∞	$\mathcal{E}_1(N)$	EOC_1	$\mathcal{E}_2(N)$	EOC_2
100	$1.0205\cdot10^{-2}$		$9.3770\cdot10^{-3}$		$6.4629\cdot10^{-3}$	
200	$2.5018\cdot10^{-3}$	2.0283	$2.2581\cdot10^{-3}$	2.0540	$1.5292\cdot10^{-3}$	2.0794
400	$6.5329\cdot10^{-4}$	1.9372	$5.8649\cdot10^{-4}$	1.9449	$3.8876\cdot10^{-4}$	1.9758
800	$1.6623\cdot10^{-4}$	1.9746	$1.4426\cdot10^{-4}$	2.0234	$9.7702\cdot10^{-5}$	1.9924
1600	$5.0943\cdot10^{-5}$	1.7062	$3.5888\cdot10^{-5}$	2.0071	$2.4118\cdot10^{-5}$	2.0183

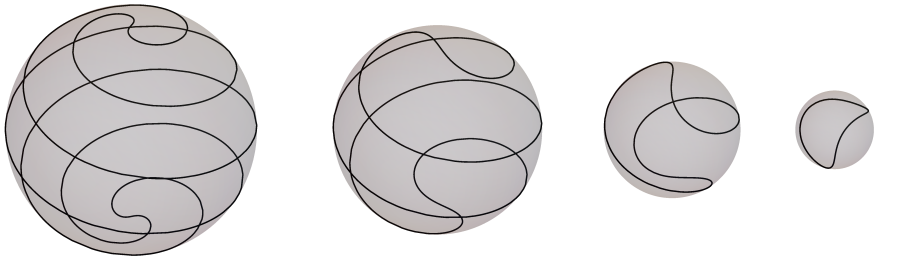

(A) $\tilde{t} = 0$ (B) $\tilde{t} = 0.15$ (C) $\tilde{t} = 0.35$ (D) $\tilde{t} = 0.45$

FIGURE 3. Results of the numerical simulation from Example 1. The discretized curve is visualized at four different time levels along with the corresponding sphere.

Example 2. The initial curve Γ_0 for the second example is given by the parametrization

$$\mathbf{X}\left(\tfrac{u}{2\pi}, 0\right) = \frac{1}{\sqrt{1 + (5\cos(10u))^2}} \begin{pmatrix} \cos u \\ \sin u \\ 5\cos(10u) \end{pmatrix}, \qquad u \in [0, 2\pi].$$

The results of the numerical simulation are presented in Table 2 and Figure 4.

8. **Conclusions.** We have compared the curvature flow of closed curves in $\mathbb{R}^m$ with a family of moving hypersurfaces and further analyzed the special case of shrinking spheres. Main Theorem allows us to bound evolving curves by a family of shrinking spheres and provides an alternative proof to the known result for evolving spherical curves. The motion of curves embedded in sphere, defined by a parametrization, was also analyzed numerically by means of a semi-implicit scheme with discretization based on osculating circles in which the second-order convergence can be observed. The accuracy can be further improved by adding a non-trivial tangential velocity for preventing local aggregation of points (see [4]).

TABLE 2. Results of the numerical computation from Example 2. The error measurements were taken during time interval $[0, 0.45]$.

N	$\mathcal{E}_\infty(N)$	EOC_∞	$\mathcal{E}_1(N)$	EOC_1	$\mathcal{E}_2(N)$	EOC_2
400	$1.1538\cdot10^{-1}$		$1.1538\cdot10^{-1}$		$1.0340\cdot10^{-1}$	
		1.9639		1.9640		2.2232
800	$2.9575\cdot10^{-2}$		$2.9574\cdot10^{-2}$		$2.2146\cdot10^{-2}$	
		2.0276		2.0280		2.0975
1200	$1.2998\cdot10^{-2}$		$1.2996\cdot10^{-2}$		$9.4608\cdot10^{-3}$	
		2.0218		2.0222		2.0547
1600	$7.2659\cdot10^{-3}$		$7.2636\cdot10^{-3}$		$5.2386\cdot10^{-3}$	
		2.0281		2.0269		2.0459
2000	$4.6211\cdot10^{-3}$		$4.6209\cdot10^{-3}$		$3.3186\cdot10^{-3}$	

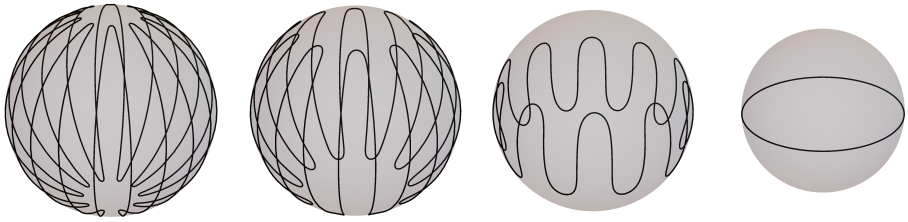

(A) $\tilde{t} = 0$ (B) $\tilde{t} = 0.01$ (C) $\tilde{t} = 0.05$ (D) $\tilde{t} = 0.2$

FIGURE 4. Results of the numerical simulation from Example 2. The discretized curve is visualized at four different time levels along with the corresponding sphere.

Acknowledgments. The first and third author were partly supported by the project No. 15-27178A of Ministry of Health of the Czech Republic, the first author was partly supported by the Foundation Nadání Josefa, Marie a Zdeňky Hlávkových, by the Study at KU Scholarship from Kanazawa University and by the project of the Student Grant Agency of the Czech Technical University in Prague No. SGS17/194/OHK4/3T/14, and the second author was partly supported by JSPS KAKENHI Grant Numbers 15H03632 and 16H03953.

REFERENCES

[1] S. J. Altschuler, Singularities for the curve shortening flow for space curves, *Journal of Differential Geometry*, **34** (1991), 491–514.

[2] S. J. Altschuler and M. A. Grayson, Shortening space curves and flow through singularities, *Journal of Differential Geometry*, **35** (1992), 283–298.

[3] L. Ambrosio and H. M. Soner, A level set approach to the evolution of surfaces of any codimension, *Journal of Differential Geometry*, **43** (1996), 693–737.

[4] M. Beneš, M. Kimura, P. Pauš, D. Ševčovič, T. Tsujikawa and S. Yazaki, Application of a curvature adjusted method in image segmentation, *Bulletin of the Institute of Mathematics, Academia Sinica (New Series)*, **3** (2008), 509–523.

[5] P. Burchard, L. T. Cheng, B. Merriman and S. Osher, Motion of curves in three spatial dimensions using a level set approach, *Journal of Computational Physics*, **170** (2001), 720–741.

[6] J. Christiansen, Numerical solution of ordinary simultaneous differential equations of the 1st order using a method for automatic step change, *Numerische Mathematik*, **14** (1970), 317–324.

[7] K. Corrales, Non existence of type II singularities for embedded and unknotted space curves, preprint, arXiv:1605.03100v1, 2016.

[8] G. Dziuk, Convergence of a semi-discrete scheme for the curve shortening flow, *Mathematical Models and Methods in Applied Sciences*, **4** (1994), 589–606.
[9] L. C. Evans and R. F. Gariepy, *Measure Theory and Fine Properties of Functions*, CRC Press, Boca Raton, FL, 1992.
[10] M. Gage and R. S. Hamilton, The heat equation shrinking convex plane curves, *Journal of Differential Geometry*, **23** (1986), 69–96.
[11] M. Grayson, The heat equation shrinks embedded plane curves to round points, *Journal of Differential Geometry*, **26** (1987), 285–314.
[12] S. He, Distance comparison principle and Grayson type theorem in the three dimensional curve shortening flow, preprint, arXiv:1209.5146v1, 2012.
[13] M. Holodniok, A. Klíč, M. Kubíček and M. Marek, *Methods of Analysis of Nonlinear Dynamical Models*, Academia Praha, 1986.
[14] G. Huisken, Flow by mean curvature of convex surfaces into spheres, *Journal of Differential Geometry*, **20** (1984), 237–266.
[15] G. Khan, A condition ensuring spatial curves develop type-II singularities under curve shortening flow, preprint, arXiv:1209.4072v3, 2015.
[16] M. Kimura, Geometry of hypersurfaces and moving hypersurfaces in $\mathbb{R}^m$ for the study of moving boundary problems, *Topics on Partial Differential Equations, Jindřich Nečas Center for Mathematical Modeling, Lecture notes*, **4** (2008), 39–93.
[17] M. Kolář, M. Beneš and D. Ševčovič, Area preserving geodesic curvature driven flow of closed curves on a surface, *Discrete and Continuous Dynamical Systems - Series B*, **22** (2017), 3671–3689.
[18] K. Mikula, Image processing with partial differential equations, *Nato Science Series*, **75** (2002), 283–322.
[19] T. Mura, *Micromechanics of Defects in Solids*, Springer Netherlands, 1987.
[20] S. Osher and J. A. Sethian, Fronts propagating with curvature dependent speed: Algorithms based on Hamilton-Jacobi formulations, *Journal of Computational Physics*, **79** (1988), 12–49.
[21] J. R. Rice and M. Mu, An experimental performance analysis for the rate of convergence of collocation on general domains, *Numerical Methods for Partial Differential Equations*, **5** (1989), 45–52.
[22] J. A. Sethian, *Level Set Methods: Evolving Interfaces in Geometry, Fluid Mechanics, Computer Vision, and Materials Science*, Cambridge University Press, 1996.
[23] A. Visintin, *Models of Phase Transitions*, Birkhäuser, Boston, 1996.
[24] Y. Y. Yang and X. X. Jiao, Curve shortening flow in arbitrary dimensional Euclidian space, *Acta Mathematica Sinica*, **21** (2005), 715–722.

Received January 2018; revised June 2018.

E-mail address: jiri.minarcik@fjfi.cvut.cz
E-mail address: mkimura@se.kanazawa-u.ac.jp
E-mail address: michal.benes@fjfi.cvut.cz